



Published in final edited form as:

Genesis. 2016 January ; 54(1): 3–18. doi:10.1002/dvg.22908.

Temporal and spatial requirements for Nodal-induced anterior mesendoderm and mesoderm in anterior neurulation

Ngawang Gonsar^{1,2,*}, Alicia Coughlin^{1,2,*}, Jessica A. Clay-Wright¹, Bethanie R. Borg¹, Lexy M. Kindt^{1,2}, and Jennifer O. Liang^{1,2,3}

¹Department of Biology, University of Minnesota Duluth

²Integrated Biosciences Graduate Program, University of Minnesota

Abstract

Zebrafish with defective Nodal signaling have a phenotype analogous to the fatal human birth defect anencephaly, which is caused by an open anterior neural tube. Previous work in our laboratory found that anterior open neural tube defects in Nodal signaling mutants were caused by defects in mesendodermal/mesodermal tissue. Defects in these mutants are already apparent at neural plate stage, before the neuroepithelium starts to fold into a tube. Consistent with this, we found that the requirement for Nodal signaling maps to mid-late blastula stages. This timing correlates with the timing of prechordal plate mesendoderm and anterior mesoderm induction, suggesting these tissues act to promote neurulation. To further identify tissues important for neurulation, we took advantage of the variable phenotypes in Nodal signaling-deficient *sqt* mutant and *Lefty1*-overexpressing embryos. Statistical analysis indicated a strong, positive correlation between a closed neural tube and presence of several mesendoderm/mesoderm-derived tissues (hatching glands, cephalic paraxial mesoderm, notochord, and head muscles). However, the neural tube was closed in a subset of embryos that lacked any one of these tissues. This suggests that several types of Nodal-induced mesendodermal/mesodermal precursors are competent to promote neurulation.

Keywords

zebrafish; Nodal; neural tube defects; anencephaly

Introduction

Neural tube defects (NTD) are among the most common human birth defects, occurring in approximately 1 in every 1000 pregnancies (Copp *et al.*, 2013). NTD are caused by failure in closure of the neural tube, the precursor to the brain and spinal cord. One of the most severe NTD is anencephaly in which the anterior neural tube fails to close, causing complete or partial absence of the developing cranial vault and cerebral hemisphere (Detrait *et al.*, 2005).

³Corresponding Author: Jennifer Liang, 1035 Kirby Drive, Rm 207, Duluth, MN 55812, 218-726-7681, joliang@d.umn.edu.
*These authors contributed equally to this work

Primary neurulation is the process that drives neural tube closure in the region that will become the brain and the majority of the spinal cord. Secondary neurulation forms the posterior-most region of the trunk spinal cord and the spinal cord of the tail. Only failures in primary neurulation cause NTD. The morphological events of primary neurulation are well conserved across many vertebrate species. Primary neurulation initiates with the columnarization of neuroectodermal cells to form the neural plate, a polarized epithelium with cells tightly bound to one another through both adherens and tight junctions (Colas and Schoenwolf, 2001; Lowery and Sive, 2004). Neural plate formation is followed by the thickening and elevation of the neural plate borders to generate the neural folds, which ultimately fuse at the dorsal midline producing a closed neural tube (Colas and Schoenwolf, 2001; Lowery and Sive, 2004). In zebrafish, there is a slight variation in this process (Colas and Schoenwolf, 2001; Kimmel *et al.*, 1995; Lowery and Sive, 2004; Schmitz and Campos-Ortega, 1994). The neural tube first forms a neural rod, in which cells of the right and left sides of the neural tube are in contact. A lumen later develops in the center of the rod to transform it into a tube.

Many human NTD are thought to have a genetic component, although the genes involved are not fully characterized (Au *et al.*, 2010; Harris and Juriloff, 2010; Juriloff and Harris, 2000). Work in genetic model organisms has the potential to identify candidate genes as well as increase understanding of the complex neurulation process. Zebrafish mutants with defective Nodal signaling exhibit NTD analogous to the human birth defect anencephaly (Aquilina-Beck *et al.*, 2007; Araya *et al.*, 2014; Lu *et al.*, 2013). Zebrafish have three Nodal ligands: Cyclops (Cyc), Squint (Sqt), and Southpaw (Schier, 2003). These ligands all signal through a receptor complex containing the One Eyed Pinhead (Oep) protein (Schier, 2003). *oep*, *sqt*, and *cyc*;*sqt* double mutants all exhibit open anterior neural tubes, as do embryos overexpressing the Nodal signaling inhibitor Lefty1 (Aquilina-Beck *et al.*, 2007; Lu *et al.*, 2013). In contrast, the posterior region of the neural tube is closed (Ciruna *et al.*, 2006). One of the primary defects in these Nodal deficient embryos appears to be lack of cell adhesion during the earliest steps of neurulation. The cells of the developing neural tube are disorganized from the neural plate stage onwards (Aquilina-Beck *et al.*, 2007; Araya *et al.*, 2014; Lu *et al.*, 2013). This disorganization is likely in part caused by decreased expression of the cell adhesion protein N-cadherin, which is required for closure of the zebrafish neural tube (Aquilina-Beck *et al.*, 2007; Lele *et al.*, 2002)

Our previous research suggested the role for Nodal signaling is not directly in the neuroepithelium, but rather in the induction of the mesendoderm and mesoderm (Aquilina-Beck *et al.*, 2007). Embryos that completely lack Nodal signaling have no anterior mesendoderm or mesoderm and always have an open neural tube (Aquilina-Beck *et al.*, 2007). In these embryos, activation of the Nodal signaling pathway cell autonomously rescued the formation of mesendodermal/mesodermal tissues and corrected the neural tube defect (Aquilina-Beck *et al.*, 2007). This suggested that the Nodal signaling pathway need not be activated in the neural tube cells, but instead has an indirect role within the mesendoderm/mesoderm. Consistent with this model, a recent study added a Nodal signaling inhibitor at 70% epiboly, after the induction of mesendoderm/mesoderm is complete, and found no effect on anterior neurulation (Araya *et al.*, 2014).

Similar to the role of the mesendoderm/mesoderm in zebrafish, the head mesenchyme in mice, which is composed of mesodermal and neural crest cells, plays an essential role in anterior neurulation (Chen and Behringer, 1995). In rodents, elevation of the cranial neural folds is preceded by the expansion of the underlying head mesenchyme (Morriss and Solursh, 1978; Solursh and Morriss, 1977; Tuckett and Morriss-Kay, 1986). Additionally, loss of function of various genes expressed in the head mesenchyme results in lethal NTD, including anencephaly. For example, the *twist* and *cart1* genes are both expressed in the head mesenchyme. Knockout of either gene reduces expansion of the cranial mesenchyme and results in NTD (Chen and Behringer, 1995; Zhao *et al.*, 1996). This led to the hypothesis that expanding head mesenchyme drives the elevation of the neural folds. The right and left neural folds subsequently converge and then fuse at the dorsal midline to form a closed neural tube. However, more characterization is needed to determine whether the anterior mesendoderm/mesoderm in zebrafish and head mesenchyme in mice have overlapping functions.

Our goal was to identify the temporal requirement for Nodal signaling in neurulation and define the areas of mesendoderm/mesoderm that have a role in neural tube closure. Consistent with the fact that the morphology of the neuroepithelium is already abnormal by neural plate stages (Aquilina-Beck *et al.*, 2007), we found that the requirement for Nodal signaling in anterior neurulation occurs up to the late blastula stages (dome stage, 4.3 hpf). This temporal requirement falls within the time when Nodal is inducing mesendoderm and mesoderm, and is before the onset of neuroepithelium formation. There was a strong statistical correlation between the presence of prechordal plate mesendoderm derivatives and head mesoderm derivatives and a closed neural tube. However, none of the tissues assayed (hatching gland, anterior notochord, cephalic paraxial mesoderm, and head muscles) were always present when the neural tube was closed, and thus their precursors were not absolutely necessary for anterior neurulation. Additionally, a correlation was observed between neural tube closure and the summed tissue presence of hatching glands and notochord. We propose a model in which Nodal signaling induces prechordal plate mesendoderm and anterior mesoderm during the blastula stages (Aquilina-Beck *et al.*, 2007). When a critical threshold of these mesendodermal/mesodermal precursors is present, they are able to interact with the overlying neuroectoderm and induce the changes that are required for neural tube closure.

Results

Temporal overlap in Nodal signaling's role in neural tube closure and mesendoderm/mesoderm induction

Our previous work suggested that Nodal signaling's role in neurulation is through the induction of mesendoderm/mesoderm or a signal produced by these tissues (Aquilina-Beck *et al.*, 2007). If this hypothesis is correct, then Nodal's temporal requirement in neurulation should occur at the same time as Nodal induction of mesendoderm/mesoderm, which occurs between 3 hpf (1000 cell stage, early blastula) and 6 hpf (shield stage, early gastrula) (Hagos and Dougan, 2007). We found that Nodal signaling is required during a subset of this time

for neural tube closure. This suggests that a subset of Nodal-dependent mesendodermal/mesodermal tissues are involved in neurulation.

To determine the temporal requirement for Nodal signaling in neurulation, we used the Nodal inhibitor SB505124, a small molecule that blocks the activity of ALK 4, 5, and 7 Nodal specific receptors (DaCosta Byfield *et al.*, 2004). In zebrafish, SB505124 treatment produces a phenotype similar to Nodal deficient embryos and causes reduced expression of Nodal-regulated genes (Hagos and Dougan, 2007; Hagos *et al.*, 2007). Because of unexpected complexities with the inhibitor, we utilized two experimental designs to determine the timing requirements of Nodal signaling. Results from both designs suggest that the requirement for Nodal signaling occurs between 3 hpf (1000 cell stage, mid blastula) and 4.3 hpf (dome stage, late blastula).

In our first experiments, embryos were exposed to a 75 or 100 μ M dose of SB505124 for 20 minutes, and then moved to a new Petri dish, resulting in at least a 1:10 dilution of SB505124. The fish were raised until ~24 hpf and then assayed for pineal morphology, which is a sensitive indicator of anterior neural tube closure (Aquilina-Beck *et al.*, 2007). An oval shaped pineal anlage indicated a closed anterior neural tube, while an elongated or divided pineal indicated an open neural tube (Fig. 1).

The majority of embryos treated with the inhibitor starting at 3.8 hpf (high oblong stage, mid blastula) and 4.0 hpf (sphere stage, mid blastula) had an open neural tube phenotype (Fig. 1, Table 1). Treatment starting at 4.3 hpf (dome stage, late blastula) resulted in embryos with both open and closed neural tubes (Fig. 1; Table 1). Initiating treatment at 4.7 hpf (30% epiboly, late blastula) consistently resulted in embryos with closed neural tubes (Fig. 1; Table 1). This suggests that 4.3 hpf is very close to the boundary between when Nodal signal is required and when it is not. The same inhibitor treatments that produced open neural tube phenotypes caused defects in mesendoderm and mesoderm formation. These defects included complete absence of dorsal mesendoderm-derived prechordal plate, decreased numbers of dorsal mesoderm-derived notochord cells, and loss of intermediate mesoderm-derived pronephric mesoderm (Fig. 2).

As part of our control experiments, we found that SB505124 activity was persisting even after extensive dilution of the inhibitor (Supplemental Fig. 1). Because these difficulties made it challenging to identify when the inhibitor was acting, we repeated the time course using an experimental design similar to previous studies (Hagos and Dougan, 2007; Terashima *et al.*, 2014). In these experiments, inhibitor was again added at different time points in development, but instead of being washed away, embryos were consistently exposed to the inhibitor up to 24 hpf when the embryos were fixed.

Using this new approach, we performed a concentration curve to determine the appropriate SB505124 concentration to consistently induce an open neural tube phenotype. We found a strong dose dependent effect of SB505124. Embryos were treated from 3.8 hpf (high oblong, mid blastula stage) through 24 hpf with concentrations ranging from 0.1 to 100 μ M. The penetrance of the open neural tube phenotype increased with increasing inhibitor concentration, producing complete penetrance at doses of 10 μ M and higher (Fig. 3; Table

2). Similarly, the number of mesoderm-derived somites decreased with increasing inhibitor concentrations (Fig. 3). At the 5 μ M concentration and higher, embryos developed a cyclopic eye phenotype (Fig. 3).

Embryos treated with 100 μ M SB505124 exhibited phenotypes more severe than *MZoep* mutants (Fig. 3). In particular, *MZoep* mutants typically have several somites in their tails. In our 100 μ M treated embryos, these somites are missing. A similar loss of tail somites was observed in embryos exposed to high doses of the related Nodal signaling inhibitor SB431542 (Sun *et al.*, 2006) and when *MZoep* embryos were treated with SB505124 (Hagos *et al.*, 2007). In these cases, the inhibitor was probably also blocking activity of Activin-like proteins, which signal through the same receptors as Nodal but do not require *Oep*.

The new experimental design using consistent inhibitor exposure produced embryos with more severe mesendodermal/mesodermal phenotypes compared to our original 20 minutes of inhibitor exposure. For example, embryos exposed to 10 μ M and 20 μ M of SB505124 from blastula stages through 24 hpf had similar phenotypes to *MZoep* mutants, which lack all Nodal signaling (Fig. 3) (Gritsman *et al.*, 1999). However, when embryos were treated for only 20 minutes, 75 μ M SB505124 treatment was needed to phenocopy *MZoep* (Fig. 1). As we also switched from SB505124 supplied by Sigma Aldrich to inhibitor supplied by Tocris, some of the difference could also be due to differences in SB505124 activity between the two suppliers.

We chose to use our highest concentration, 100 μ M SB505124, in our subsequent experiments to ensure effective inhibition of Nodal signaling. Despite the change in treatment time from 20 minutes to over 20 hours and the change in supplier of the inhibitor, the timing of effect on neural tube closure remained the same (Fig. 4, Table 3). The timing also remained the same when 20 μ M SB505124 was used, suggesting any inhibition of Activin-like proteins at the 100 μ M dose was not contributing to the neural tube phenotype (Supplemental Table 1). In all cases, treatment starting at 4.3 or earlier caused open neural tubes, while treatment starting 4.7 or later did not (Fig. 1 and 4, Tables 1 and 3, Supplemental Table 1).

There was also an almost exact match between open neural tube defects and decreased expression of mesendodermal/mesodermal markers (Supplemental Fig. 2, Supplemental Table 2). For instance, all embryos treated with SB505124 starting at 3.8 hpf (high oblong stage, mid blastula) or 4.0 hpf (sphere stage, mid blastula) had open neural tubes as expected and lacked all or almost all expression of mesendodermal/mesodermal markers (Supplemental Fig. 2, Supplemental Table 2). Treatment starting at 4.3 hpf (dome stage, late blastula) caused mixed neural tube and mesendodermal/mesodermal phenotypes while treatment at or after 4.7 hpf (30% epiboly, late blastula) resulted in closed neural tube phenotypes and a much milder defect of mesendodermal/mesodermal tissues.

Absence of head mesendodermal/mesodermal tissues correlates with open neural tube phenotype

With the goal of identifying specific regions of the head mesendoderm and anterior mesoderm required for neural tube closure, we used *sqt* mutants and *Lefty1* overexpressing

embryos in a correlative approach. These embryos have variable mesendoderm/mesoderm and neural tube phenotypes (Aquilina-Beck *et al.*, 2007; Thisse *et al.*, 2000). Four tissues were assayed, including the prechordal plate mesendoderm-derived hatching glands, mesoderm-derived anterior notochord, cephalic paraxial mesoderm, and mesendoderm and mesoderm-derived head muscles (Fig. 5). If the precursors to an anterior mesendodermal/mesodermal tissue are required for neurulation, then they should always be present when the neural tube is closed and always absent when the neural tube is open. We found there was a strong correlation between the presence of each head mesendodermal/mesodermal tissue and a closed neural tube phenotype.

The hatching glands are derived from the anterior most prechordal plate, which is the first mesendodermal tissue to involute during gastrulation (Thisse *et al.*, 1994; Vogel and Gerster, 1997). The prechordal plate underlies the presumptive anterior neuroectoderm during gastrulation, when specification of the neuroectoderm is initiated (Schmidt *et al.*, 2013). Hence, precursors to the hatching glands were strong candidates to be influencing neurulation. Embryos were categorized into four groups based on whether the hatching gland tissue was present or absent and whether the neural tube was open or closed (Fig. 6, Supplemental Fig. 3). To assess the correlation, we calculated the ϕ coefficient. $\phi=1$ indicated an absolute positive correlation between a closed neural tube and hatching gland presence, and $\phi=-1$ indicated an absolute negative correlation. A one-tailed Fisher's exact test was used to determine whether a correlation was statistically significant. This analysis indicated a positive correlation between neural tube closure and hatching gland presence that reached significance only in the *Lefty1* overexpressing embryos (*sqt*: $\phi=0.2566$; $P=0.26$; *lefty1* mRNA injected: $\phi=0.61$; $P=0.000086$).

Notochord precursors are also in close proximity to the anterior neuroepithelium during early development, suggesting they could also influence closure of the anterior neural tube (Kimmel *et al.*, 1990; Solnica-Krezel and Sepich, 2012). Consistent with this, there was a statistically significant positive correlation between presence of anterior notochord and a closed neural tube (*sqt* $\phi=0.39$; $P=5.4 \times 10^{-4}$; *lefty1* mRNA injected $\phi=0.49$; $P=4.6 \times 10^{-9}$) (Fig. 6; Supplemental Fig. 4).

The cephalic paraxial mesoderm (cpm) serves as the primary precursor to all cranial skeletal muscles and the pharyngeal arches. Mouse *twist* mutants that have a disorganized cpm, display open cranial neural tubes, suggesting a potential role for cpm in vertebrate neurulation (Chen and Behringer, 1995). As with the other tissues tested, cpm presence had a strong positive correlation with a closed neural tube (*sqt* $\phi=0.42$, $P=8.1 \times 10^{-4}$; *lefty1* mRNA injected $\phi=0.67$, $P=2.5 \times 10^{-6}$) (Fig. 7; Supplemental Fig. 5).

Anterior mesendodermal/mesodermal-derived head muscles had the lowest correlation with neural tube closure of the tissues assayed (Fig. 8; Supplemental Table 3). Developing head muscles become apparent at approximately 50 hpf, during the hatching period, and give rise to the eye, jaw, and gill arch muscles in the adult (Kimmel *et al.*, 1990). We found a strong relationship between head muscles in *lefty1* mRNA injected embryos ($\phi=0.40$, $P=0.024$), but only a weak correlation in *sqt* ($\phi=0.10$; $P=0.52$).

Despite the positive correlation between each mesendodermal/mesodermal tissue tested and neural tube closure, none had an absolute correlation. For each tissue, there were a subset of Nodal deficient embryos that completely lacked the tissue and had a closed anterior neural tube, and others that had the tissue but an open anterior neural tube (Fig. 6–8, Supplemental Fig. 3–5, Supplemental Table 3). This suggests that none of the specific precursor populations that give rise to each of the four assayed tissues is essential for driving the process of neurulation.

As a final test, we assayed the same mesendodermal/mesodermal tissues in *cyc* mutants, which lack one of the zebrafish Nodal ligands, and *casanova* (*cas*) mutants, which lack a transcription factor required for endoderm development. Both mutants always have a closed neural tube (Fig. 9) (Aquilina-Beck *et al.*, 2007; Liang *et al.*, 2000). Consistent with their normal anterior neurulation, both mutants also had hatching gland, notochord, and cpm tissues that were indistinguishable from WT siblings (Fig. 9).

Correlation with amount of mesendodermal/mesodermal tissue and neural tube closure

Based on our correlative study findings, we hypothesized a minimum threshold of mesendodermal/mesodermal tissue presence was required to drive anterior neural tube closure. To test this, we analyzed *sqt* mutant embryos and wildtype embryos treated with SB505124 at 4.3 hpf (dome stage, late blastula) for pineal morphology and for presence of hatching gland and notochord, this time scoring the whole length of embryo for notochord. Presence of each tissue type was scored on a 0 to 3 scale, with 0 indicating complete absence and 3 indicating normal levels. Hatching gland and notochord scores were summed for individual embryos to calculate a total tissue presence score that ranged from 0 to 6.

There was a significant correlation between neural tube closure and total tissue presence. The most common among all of the embryos was 1 (n=315/477) (Fig. 10, Supplemental Fig. 6). Embryos with an open neural tube phenotype had total score of 0–2, while those with a closed had a range of 1–5 (Figure 10). A two-tailed Fisher's exact test indicated a positive correlation between total tissue presence and neural tube closure when the two types of Nodal deficient embryos were grouped together or considered separately (combined SB505124 treated and *sqt* mutant datasets, $P=2.2 \times 10^{-16}$; SB505124 treated alone $P=2.2 \times 10^{-16}$; *sqt* mutants alone, $P=0.01161$). Thus, the chance of neural tube closure increased when there was more notochord and hatching gland. These data suggest there is a minimum threshold of total mesendodermal/mesodermal precursors required to support neural tube closure.

Discussion

In this study, we established the temporal requirement for Nodal signaling and mapped regions of mesendoderm and mesoderm important for anterior neurulation. We found Nodal signaling in neural tube closure was required through late blastula stages (4.3 hpf) and overlapped with a subset of the time Nodal induces mesendoderm/mesoderm (Hagos and Dougan 2007). Further, our data suggest that a wide range of mesendodermal/mesodermal precursors is competent to promote anterior neurulation. Although there was a strong correlation between the presence of multiple mesendodermal/mesodermal tissues and a

closed neural tube, none of the tissues were always present when the neural tube was closed or always absent when the neural tube was open. However, a closed neural tube correlated with the amount of mesendodermal/mesodermal tissue present. These data suggest a model in which a critical amount of Nodal-induced mesendoderm/mesoderm precursor cells are required to make the developing anterior neuroectoderm competent to undergo the process of neurulation. The timing of sensitivity to the Nodal inhibitor and the abnormalities of the neural tube observed at the onset of neurulation in embryos that completely lack Nodal signaling (Aquilina-Beck *et al.*, 2007; Araya *et al.*, 2014) suggests these precursors act in a very early step in the formation of the neural plate epithelium.

Nodal acts during blastula stages to induce the mesendodermal/mesodermal tissues required for neural tube closure

We found Nodal signaling was required for anterior neurulation up to late blastula stages (up to 4.3 hpf). Treatment with even very high levels of Nodal inhibitor after this time period did not cause NTD, although the inhibitor was still effective, as embryos whose treatment started at early gastrula stage (5.3 hpf, 50% epiboly stage) had cyclopia. The timing of inhibitor sensitivity falls within the time period when mesoderm, endoderm, and mesendoderm are being induced, supporting the model that the role of Nodal signaling in neurulation is through the induction of mesendoderm/mesoderm. Endoderm is not included in this model because *cas* mutants, which completely lack endoderm, always have a closed neural tube (Liang *et al.*, 2000). However, it is possible that the endoderm plays a redundant role with mesoderm and mesendoderm to promote neural tube closure.

Nodal signals also have direct roles in patterning the neural tube. For instance, in zebrafish, Nodal is required for the development of the ventral neural tube (ventral brain and floor plate of the spinal cord) (Hatta *et al.*, 1991; Rebagliati *et al.*, 1998; Sampath *et al.*, 1998). In some cases, the ventral neural tube acts as a hinge point that bends the neural tube so that it can close. We can rule out an essential role for ventral neural tube in zebrafish neurulation, as *cyc* mutants, which have no ventral brain or spinal cord, have a closed neural tube (Figure 9) (Liang *et al.*, 2000). It is also unlikely that the neural tube is open due to a lack of another neural tissue. The SB505124 sensitive period is over before neural induction has begun and treatment with a related Nodal signaling inhibitor (SB431542) at 70% epiboly, just before the neural plate begins forming, does not cause NTD (Araya *et al.*, 2014). Further, the pattern of gene expression in the developing neural tube (with the exception of ventral neural tube markers) is remarkably normal in MZ*oep* embryos, suggesting most tissues are present (Aquilina-Beck *et al.*, 2007; Mathieu *et al.*, 2002).

The period in which SB505124 causes open neural tubes is also consistent with studies of Zygotic *oep* (*Zoep*) mutants, which suggests that Nodal is acting near the onset of zygotic transcription (1000 cell stage, or around 2.75 hpf), within the period when SB505124 caused NTD. *Zoep* embryos can have either closed or open neural tubes (Aquilina-Beck *et al.*, 2007; Lu *et al.*, 2013). The onset of zygotic transcription can vary slightly from one embryo to another (Tadros and Lipshitz, 2009). Thus, a likely explanation of the incomplete penetrance of the NTD is that some *Zoep* embryos might have persistence of maternally-

derived Oep or a slightly earlier onset of zygotic transcription, resulting in sufficient Oep protein during the period when Nodal is required for neurulation.

We used two different experimental designs to determine the temporal requirement for Nodal signaling in anterior neural tube closure. Even though the first embryos were exposed to high doses of Nodal signaling inhibitor for 20 minutes and the second to high doses for ~20 hours, both identified the same temporal requirement. One possibility for the effectiveness of the short treatment is the fact that Nodal signals act in a positive feedback loop that positively regulate their own transcription. We know from our washing experiments that a small amount of inhibitor persisted in the embryos treated for only 20 minutes. Thus, one possible explanation is that after a short treatment at high concentrations, only a minimal amount of SB505124 was needed to inhibit the small amount of remaining Nodal signaling. Another possibility is that the embryos sequestered SB505124 so that high concentrations persisted within the embryo even after washing.

Broad region of mesendoderm and mesoderm is important for anterior neural tube closure

Our data strongly suggests that a large region of anterior mesendoderm/mesoderm is capable of interacting with the overlying neuroectoderm to promote neural tube closure. Our favorite model is that a critical amount of anterior mesendoderm/mesoderm tissue is required for anterior neurulation. When the amount drops below this threshold, the embryo develops NTD. In support of this model, we found a correlation between neural tube closure and the total combined presence of the mesendodermal/mesodermal tissues hatching gland and notochord in *sqt* mutant and 4.3 hpf SB505124 treated embryos. There was a strong dose dependent effect. With increasing total tissue scores, the likelihood of an embryo having a closed neural tube phenotype increased after the score of 1 (either a small amount of hatching gland tissue or a small amount of notochord tissue). It is interesting that embryos with a combined score of 1 could have either open or closed neural tubes. The most likely explanation is that these embryos differed in the presence of other mesendodermal tissues we did not test.

From our study, we cannot rule out the alternative possibility that a specific region of mesendoderm/mesoderm that we did not test is the key tissue required for neural tube closure. The precursors to the tissues analyzed in this study were the most likely to be involved in neurulation due to their spatial proximity or length of contact with the presumptive anterior neural tube. It is possible that the analyzed tissues correlated with a closed neural tube not because they were involved, but because they were co-induced by Nodal along with such a specific, key tissue. The presence of such a tissue is improbable, as we tested tissues that spanned the range of anterior mesendoderm/mesoderm derivatives.

We do not yet know the mechanisms by which mesendodermal/mesodermal tissues promote anterior neurulation. One possibility is that there is a biochemical signal that is secreted by a large range of mesendodermal/mesodermal tissues. If adequate numbers of mesendodermal/mesodermal cells are present, then enough of this signal is produced to drive neural tube closure. Consistent with this possibility, a large region of the head mesendoderm/mesoderm is in close proximity to the overlying anterior neuroectoderm (Kimmel *et al.*, 1990; Solnica-Krezel and Sepich, 2012). At the start of gastrulation, the mesendodermal cells move inward

through the blastopore, forming a lining beneath the future neuroectodermal cells and the yolk cell below (Solnica-Krezel and Sepich, 2012). Contact between the germ layers persists until they undergo further specification around the end of gastrulation. Thus, the head mesendoderm/mesoderm is within a few cell diameters of the overlying neuroectoderm prior to and during anterior neurulation.

There are other examples of neural patterning events where a wide range of mesendodermal/mesodermal tissues are involved. For instance, Engrailed (En) proteins have a prominent role in midbrain and anterior hindbrain development (Joyner, 1996). In *Xenopus* explants, anterior notochord tissue acted as a strong inducer of En-2 in ectodermal tissue, demonstrating that it had been induced to form an anterior neural fate. However, the presumptive head mesoderm and anterior somites could induce En-2 expression, although not as efficiently (Hemmati-Brivanlou *et al.*, 1990). A similar redundant system could explain why absence of any one tissue was not sufficient to cause anterior NTD in zebrafish embryos.

In mice, the head mesenchyme, which is composed of anterior mesodermal and neural crest cells, is required for anterior neurulation. It has been proposed that proliferation and expansion of the underlying head mesenchyme drives the lateral edges of the neural plate toward each other (Chen and Behringer, 1995; Harris and Juriloff, 2007, 2010). However, it is improbable that head mesendoderm/mesoderm proliferation drives neural tube closure in zebrafish. In contrast to other vertebrates, primary neurulation in zebrafish results from the thickening and then ‘sinking’ of the neural plate (Lowery and Sive, 2004). It is hard to reconcile proliferation of the underlying mesenchyme/mesendoderm causing this ‘sinking’ morphological event in zebrafish, as it is unlikely to be driven by an external force.

Consistent with our model that the interaction between mesendoderm/mesoderm with anterior neuroectoderm is driven by a secreted protein, there is growing evidence for signals that mediate communication between anterior neuroectoderm and underlying mesoderm-related tissue. Disruptions of approximately 70 genes in mice result in either spina bifida or exencephaly (Harris and Juriloff, 2007, 2010). Many of these genes encode secretory proteins that have functions including involvement in biochemical cell-cell signaling pathways (ex. Sonic Hedgehog, Fibroblast Growth Factors, and Wingless Integrated) (Harris and Juriloff, 2007, 2010; Londin *et al.*, 2005; Yamamoto *et al.*, 2003; Ybot-Gonzalez *et al.*, 2002). Additionally, many of these secreted proteins are highly expressed before and during anterior neurulation in the neuroepithelium and in adjacent tissues such as the head mesenchyme (Harris and Juriloff, 2007, 2010). These signals are potential candidates for mediating a biochemical interaction between the anterior mesendoderm/mesoderm and the anterior neural tube.

Methods

All protocols using animals were approved by the U of MN Institutional Animal Care and Use Committee.

Zebrafish stocks

Zebrafish were maintained as per standard protocols at a constant temperature of 28.5 °C in a 14:10 light:dark cycle (Westerfield, 2000). The stocks used were WT strain Zebrafish *Danio rerio* (ZDR) (Aquatica Tropical, Plant City, FL), and fish carrying the *sqt*^{cz35} (Feldman *et al.*, 1998), *cyc*^{m294} (Schier *et al.*, 1996), or *casanova*^{ta56} (*cas*) (Chen *et al.*, 1996) mutations. WT, *cyc*, and *cas* embryos were incubated at 28.5 °C and *sqt* embryos were incubated at 34 °C to increase the penetrance of the open neural tube phenotype (Hagos and Dougan, 2007; Lu *et al.*, 2013). All embryonic stages were defined morphologically (Kimmel *et al.*, 1995).

SB505124 treatment

For the short term treatment experiments, 3 hpf (1000-cell stage) ZDR embryos were dechorionated with 2mg/ml Pronase (Roche) using established methods (Link *et al.*, 2006; Westerfield, 2000). Embryos not fully dechorionated by the Pronase solution were dechorionated through gentle agitation with forceps. Post pronase treatment, embryos were always transferred using Sigma Cote (Sigma Aldrich) coated glass pipettes to prevent damage. At the desired morphological stage, embryos were exposed to 50, 75, or 100 µM of 2-(5-benzo [1,3] dioxol-5-yl-2-terbutyl-3H-imidazol-4-yl)-6-methylpyridine hydrochloride hydrate (SB505124) (Sigma Aldrich) at room temperature (Hagos and Dougan, 2007; Hagos *et al.*, 2007). All inhibitor experiments used a freshly prepared 10mM SB505124 stock in DMSO. After 20 minutes of SB505124 treatment, embryos were transferred to a Petri dish with ~10 ml of new embryo media. Post SB505124 exposure, embryos were incubated at 28.5 °C until the desired stage, then fixed and assayed.

In the long treatment experiments, we switched to Tocris as a supplier of SB505124, as we had difficulties with differences in activity among lots of the Sigma inhibitor. In these experiments, ZDR embryos were treated at specific morphological stages with the indicated doses or with 100 µM of SB505124 (Tocris) at 28.5 °C until fixation at approximately 24 hpf. We found no difference in SB505124 effectiveness between experiments where the chorions were on or off. Therefore, some experimental trials used dechorionated embryos and others used embryos still in their chorions. The dechorionated embryos were produced by treatment with 2 mg/ml Pronase at the 64 cell stage for ~7 minutes at 28.5 °C.

Whole mount RNA in situ hybridization (WISH)

Embryos were assayed by RNA whole mount in situ hybridization using established methods (Thisse and Thisse, 2014). Digoxigenin antisense RNA probes included *orthodenticle homobox 5 (otx5)* (Gamse *et al.*, 2002), *cathepsin L 1b (ctsl1b)* (Vogel and Gerster, 1997), *paired box gene 2.1 (pax 2.1)* (Pfeffer *et al.*, 1998), *floating head (flh)* (Talbot *et al.*, 1995), *goosecoid (gsc)* (Stachel *et al.*, 1993), *collagen type IX alpha 2 (col9a2)* (Thisse *et al.*, 2001), *collagen type 2 alpha-1a (col2a1)* (Yan *et al.*, 1995), *sonic hedgehog (shh)* (Krauss *et al.*, 1993) and *smooth muscle myosin heavy chain 2 (smyhc2)* (Elworthy *et al.*, 2008).

PCR genotyping

sqt heterozygotes were identified by natural breeding or by Polymerase Chain Reaction (PCR) using *sqt*^{cz35} specific primers on DNA extracted from fin clips. The shared forward primer was 5'-GAGCTTTATTTCAATAACTGCGTG-3'. The reverse primer to detect the insertion in the *sqt* mutants was 5'-ATATAAAATCAGTACAACCGCCCG-3', and the reverse primer to detect the WT allele was 5'-GCCAGCTGCTCGCATTTTATTCC-3' (Feldman *et al.*, 1998).

Photography

Bright field images were taken with a SPOT Insight Fire Wire camera mounted on a Nikon Eclipse 80i microscope. All images were processed using Adobe InDesign CS6 and minor adjustments for clarity were made using Adobe Photoshop CS6 (Adobe Systems Inc.).

mRNA injections

One to two celled stage ZDR embryos were pressure injected with 0.38–2.5 pg of *lefty1* mRNA using Harvard Apparatus PL190-nitrogen driven pico-injector. Embryos were maintained at 28.5 °C and then fixed and assayed by light microscopy and WISH. Uninjected or GFP mRNA injected sibling embryos served as controls.

Data analyses

Embryos were exposed to SB505124 beginning at several blastula stages and assayed for pineal morphology through WISH. Each dataset was organized into an appropriately sized contingency table with cells corresponding to neural tube phenotype, open or closed, and initiation of inhibitor treatment. In addition, embryos were treated SB505124 concentrations ranging from 0 μM to 100 μM and evaluated for pineal morphology with WISH. Concentration scores were placed in an 8 × 2 contingency table with cells corresponding to neural tube phenotype and SB505124 concentration. A two-tailed Fisher's exact test was used to test for association between stage at onset of inhibitor exposure and neural tube closure or SB505124 concentration and neural tube closure. Sample sizes were considered to be sufficient if a significant association (P<0.05) was observed. Analyses were performed with R version 3.1.2 software.

Homozygous *sqt*, *cyc*, *cas*, and *lefty1* mRNA injected embryos were assayed by WISH for the presence of mesendodermal and mesodermal tissues and pineal morphology. The embryos were categorized into 4 groups: mesendodermal/mesodermal tissue present and elongated or divided pineal (open NT), mesendodermal/mesodermal tissue absent and open NT, mesendodermal/mesodermal tissue present and closed NT and mesendodermal/mesodermal tissue absent and closed NT. Tissue was counted as present if there was either partial or full expression of the mesendodermal/mesodermal marker. These groups corresponded to the four quadrants within a 2 × 2 contingency table of a one-tailed Fisher's exact test, analyzed using R version 3.1.2 software. If a statistically significant relationship was observed (P<0.05), the strength of the correlation between neural tube closure and mesendodermal/mesodermal tissue presence was determined through the Phi Coefficient (ϕ).

For co-analysis of hatching glands, notochord, and pineal morphology, *sqt* mutant embryos and ZDR embryos treated with SB505124 from the 4.3 hpf (dome stage, late blastula) until they were fixed at 24 hpf and processed for WISH. Embryos were scored for hatching gland and notochord tissue presence within the same embryo using the following scores: 0 equaling tissue absent, 1 equaling some tissue present, 2 equaling most tissue present, and 3 equaling full tissue present. A two-tailed Fisher's exact test was performed using R version 3.1.2 software to test for association between the sum of hatching gland and notochord presence with neural tube closure. Summed tissue presence scores, 0 through 6, and neural tube phenotype, open or closed, corresponded to the cells of a 7×2 contingency table. Association was considered significant if $P < 0.05$.

Supplementary Material

Refer to Web version on PubMed Central for supplementary material.

Acknowledgments

This work was supported in part by an NIH grant 1 R15 HD068176-01A1 (J.O.L.) and a University of Minnesota Grant-in-Aid of Research, Artistry, and Scholarship (J.O.L.). The authors thank Adelle Schumann, Michael Schoenenberger, Jenna Ruzich, Derek Laux, Thu Tran, and Kaaren Westberg for technical assistance, Dr. Timothy Craig for guidance on the statistical analysis, and Dr. Stone Elworthy for the *smyhc2* expression plasmid.

References

- Aquilina-Beck A, Ilagan K, Liu Q, Liang JO. Nodal signaling is required for closure of the anterior neural tube in zebrafish. *BMC Dev Biol.* 2007; 7:126. [PubMed: 17996054]
- Araya C, Tawk M, Girdler GC, Costa M, Carmona-Fontaine C, Clarke JD. Mesoderm is required for coordinated cell movements within zebrafish neural plate in vivo. *Neural Dev.* 2014; 9:9. [PubMed: 24755297]
- Au KS, Ashley-Koch A, Northrup H. Epidemiologic and genetic aspects of spina bifida and other neural tube defects. *Dev Disabil Res Rev.* 2010; 16:6–15. [PubMed: 20419766]
- Chen JN, Haffter P, Odenthal J, Vogelsang E, Brand M, van Eeden FJ, Furutani-Seiki M, Granato M, Hammerschmidt M, Heisenberg CP, Jiang YJ, Kane DA, Kelsh RN, Mullins MC, Nusslein-Volhard C. Mutations affecting the cardiovascular system and other internal organs in zebrafish. *Development.* 1996; 123:293–302. [PubMed: 9007249]
- Chen ZF, Behringer RR. *twist* is required in head mesenchyme for cranial neural tube morphogenesis. *Genes Dev.* 1995; 9:686–699. [PubMed: 7729687]
- Ciruna B, Jenny A, Lee D, Mlodzik M, Schier AF. Planar cell polarity signalling couples cell division and morphogenesis during neurulation. *Nature.* 2006; 439:220–224. [PubMed: 16407953]
- Colas JF, Schoenwolf GC. Towards a cellular and molecular understanding of neurulation. *Dev Dyn.* 2001; 221:117–145. [PubMed: 11376482]
- Copp AJ, Stanier P, Greene ND. Neural tube defects: recent advances, unsolved questions, and controversies. *Lancet Neurol.* 2013; 12:799–810. [PubMed: 23790957]
- DaCosta Byfield S, Major C, Laping NJ, Roberts AB. SB-505124 is a selective inhibitor of transforming growth factor-beta type I receptors ALK4, ALK5, and ALK7. *Mol Pharmacol.* 2004; 65:744–752. [PubMed: 14978253]
- Detrait ER, George TM, Etchevers HC, Gilbert JR, Vekemans M, Speer MC. Human neural tube defects: developmental biology, epidemiology, and genetics. *Neurotoxicol Teratol.* 2005; 27:515–524. [PubMed: 15939212]
- Elworthy S, Hargrave M, Knight R, Mebus K, Ingham PW. Expression of multiple slow myosin heavy chain genes reveals a diversity of zebrafish slow twitch muscle fibres with differing requirements for Hedgehog and Prdm1 activity. *Development.* 2008; 135:2115–2126. [PubMed: 18480160]

- Feldman B, Gates MA, Egan ES, Dougan ST, Rennebeck G, Sirotkin HI, Schier AF, Talbot WS. Zebrafish organizer development and germ-layer formation require nodal-related signals. *Nature*. 1998; 395:181–185. [PubMed: 9744277]
- Gamse JT, Shen YC, Thisse C, Thisse B, Raymond PA, Halpern ME, Liang JO. Otx5 regulates genes that show circadian expression in the zebrafish pineal complex. *Nat Genet*. 2002; 30:117–121. [PubMed: 11753388]
- Gritsman K, Zhang J, Cheng S, Heckscher E, Talbot WS, Schier AF. The EGF-CFC protein one-eyed pinhead is essential for nodal signaling. *Cell*. 1999; 97:121–132. [PubMed: 10199408]
- Hagos EG, Dougan ST. Time-dependent patterning of the mesoderm and endoderm by Nodal signals in zebrafish. *BMC Dev Biol*. 2007; 7:22. [PubMed: 17391517]
- Hagos EG, Fan X, Dougan ST. The role of maternal Activin-like signals in zebrafish embryos. *Dev Biol*. 2007; 309:245–258. [PubMed: 17692308]
- Harris MJ, Juriloff DM. Mouse mutants with neural tube closure defects and their role in understanding human neural tube defects. *Birth Defects Res A Clin Mol Teratol*. 2007; 79:187–210. [PubMed: 17177317]
- Harris MJ, Juriloff DM. An update to the list of mouse mutants with neural tube closure defects and advances toward a complete genetic perspective of neural tube closure. *Birth Defects Res A Clin Mol Teratol*. 2010; 88:653–669. [PubMed: 20740593]
- Hatta K, Kimmel CB, Ho RK, Walker C. The cyclops mutation blocks specification of the floor plate of the zebrafish central nervous system. *Nature*. 1991; 350:339–341. [PubMed: 2008211]
- Joyner AL. Engrailed, Wnt and Pax genes regulate midbrain--hindbrain development. *Trends Genet*. 1996; 12:15–20. [PubMed: 8741855]
- Juriloff DM, Harris MJ. Mouse models for neural tube closure defects. *Hum Mol Genet*. 2000; 9:993–1000. [PubMed: 10767323]
- Kimmel CB, Ballard WW, Kimmel SR, Ullmann B, Schilling TF. Stages of Embryonic Development of the Zebrafish. *Developmental Dynamics*. 1995; 203:253–310. [PubMed: 8589427]
- Kimmel CB, Warga RM, Schilling TF. Origin and organization of the zebrafish fate map. *Development*. 1990; 108:581–594. [PubMed: 2387237]
- Krauss S, Concordet JP, Ingham PW. A functionally conserved homolog of the *Drosophila* segment polarity gene *hh* is expressed in tissues with polarizing activity in zebrafish embryos. *Cell*. 1993; 75:1431–1444. [PubMed: 8269519]
- Lele Z, Folchert A, Concha M, Rauch GJ, Geisler R, Rosa F, Wilson SW, Hammerschmidt M, Bally-Cuif L. parachute/n-cadherin is required for morphogenesis and maintained integrity of the zebrafish neural tube. *Development*. 2002; 129:3281–3294. [PubMed: 12091300]
- Liang JO, Etheridge A, Hantsoo L, Rubinstein AL, Nowak SJ, Izpisua Belmonte JC, Halpern ME. Asymmetric nodal signaling in the zebrafish diencephalon positions the pineal organ. *Development*. 2000; 127:5101–5112. [PubMed: 11060236]
- Link V, Shevchenko A, Heisenberg CP. Proteomics of early zebrafish embryos. *BMC Dev Biol*. 2006; 6:1. [PubMed: 16412219]
- Londin ER, Niemiec J, Sirotkin HI. Chordin, FGF signaling, and mesodermal factors cooperate in zebrafish neural induction. *Dev Biol*. 2005; 279:1–19. [PubMed: 15708554]
- Lowery LA, Sive H. Strategies of vertebrate neurulation and a re-evaluation of teleost neural tube formation. *Mech Dev*. 2004; 121:1189–1197. [PubMed: 15327780]
- Lu PN, Lund C, Khuansuwan S, Schumann A, Harney-Tolo M, Gamse JT, Liang JO. Failure in closure of the anterior neural tube causes left isomerization of the zebrafish epithalamus. *Dev Biol*. 2013; 374:333–344. [PubMed: 23201575]
- Morriss GM, Solursh M. Regional differences in mesenchymal cell morphology and glycosaminoglycans in early neural-fold stage rat embryos. *J Embryol Exp Morphol*. 1978; 46:37–52. [PubMed: 702034]
- Murakami T, Hijikata T, Matsukawa M, Ishikawa H, Yorifuji H. Zebrafish protocadherin 10 is involved in paraxial mesoderm development and somitogenesis. *Dev Dyn*. 2006; 235:506–514. [PubMed: 16261626]

- Pfeffer PL, Gerster T, Lun K, Brand M, Busslinger M. Characterization of three novel members of the zebrafish Pax2/5/8 family: dependency of Pax5 and Pax8 expression on the Pax2.1 (noi) function. *Development*. 1998; 125:3063–3074. [PubMed: 9671580]
- Rebagliati MR, Toyama R, Haffter P, Dawid IB. cyclops encodes a nodal-related factor involved in midline signaling. *Proc Natl Acad Sci U S A*. 1998; 95:9932–9937. [PubMed: 9707578]
- Sampath K, Rubinstein AL, Cheng AM, Liang JO, Fekany K, Solnica-Krezel L, Korzh V, Halpern ME, Wright CV. Induction of the zebrafish ventral brain and floorplate requires cyclops/nodal signalling. *Nature*. 1998; 395:185–189. [PubMed: 9744278]
- Schier AF. Nodal signaling in vertebrate development. *Annu Rev Cell Dev Biol*. 2003; 19:589–621. [PubMed: 14570583]
- Schier AF, Neuhauss SC, Harvey M, Malicki J, Solnica-Krezel L, Stainier DY, Zwartkruis F, Abdelilah S, Stemple DL, Rangini Z, Yang H, Driever W. Mutations affecting the development of the embryonic zebrafish brain. *Development*. 1996; 123:165–178. [PubMed: 9007238]
- Schmidt R, Strahle U, Scholpp S. Neurogenesis in zebrafish - from embryo to adult. *Neural Dev*. 2013; 8:3. [PubMed: 23433260]
- Schmitz B, Campos-Ortega J. Dorsal-ventral polarity of the zebrafish embryo is distinguishable prior to the onset of gastrulation. *Roux's archives of developmental biology*. 1994; 203:374–380.
- Solnica-Krezel L, Sepich DS. Gastrulation: making and shaping germ layers. *Annu Rev Cell Dev Biol*. 2012; 28:687–717. [PubMed: 22804578]
- Solursh M, Morriss GM. Glycosaminoglycan synthesis in rat embryos during the formation of the primary mesenchyme and neural folds. *Dev Biol*. 1977; 57:75–86. [PubMed: 863113]
- Stachel SE, Grunwald DJ, Myers PZ. Lithium perturbation and goosecoid expression identify a dorsal specification pathway in the pregastrula zebrafish. *Development*. 1993; 117:1261–1274. [PubMed: 8104775]
- Sun Z, Jin P, Tian T, Gu Y, Chen YG, Meng A. Activation and roles of ALK4/ALK7-mediated maternal TGFbeta signals in zebrafish embryo. *Biochem Biophys Res Commun*. 2006; 345:694–703. [PubMed: 16696945]
- Tadros W, Lipshitz HD. The maternal-to-zygotic transition: a play in two acts. *Development*. 2009; 136:3033–3042. [PubMed: 19700615]
- Talbot WS, Trevarrow B, Halpern ME, Melby AE, Farr G, Postlethwait JH, Jowett T, Kimmel CB, Kimelman D. A homeobox gene essential for zebrafish notochord development. *Nature*. 1995; 378:150–157. [PubMed: 7477317]
- Terashima AV, Mudumana SP, Drummond IA. Odd skipped related 1 is a negative feedback regulator of nodal-induced endoderm development. *Dev Dyn*. 2014; 243:1571–1580. [PubMed: 25233796]
- Thisse B, Pfumio S, Furthauer M, Loppin B, Heyer V, Degraeve A, Woehl R, Lux A, Steffan T, Charbonnier XQ, Thisse C. Expression of the zebrafish genome during embryogenesis. *ZFIN Direct Data Submission*. 2001
- Thisse B, Thisse C. In situ hybridization on whole-mount zebrafish embryos and young larvae. *Methods Mol Biol*. 2014; 1211:53–67. [PubMed: 25218376]
- Thisse B, Wright CV, Thisse C. Activin- and Nodal-related factors control antero-posterior patterning of the zebrafish embryo. *Nature*. 2000; 403:425–428. [PubMed: 10667793]
- Thisse C, Thisse B, Halpern ME, Postlethwait JH. Goosecoid expression in neurectoderm and mesendoderm is disrupted in zebrafish cyclops gastrulas. *Dev Biol*. 1994; 164:420–429. [PubMed: 8045345]
- Tuckett F, Morriss-Kay GM. The distribution of fibronectin, laminin and entactin in the neurulating rat embryo studied by indirect immunofluorescence. *J Embryol Exp Morphol*. 1986; 94:95–112. [PubMed: 3531379]
- Vogel AM, Gerster T. Expression of a zebrafish cathepsin L gene in anterior mesendoderm and hatching gland. *Deve Genes Evol*. 1997; 206:477–479.
- Westerfield, M. *The zebrafish book*. 2000.
- Yamamoto S, Hikasa H, Ono H, Taira M. Molecular link in the sequential induction of the Spemann organizer: direct activation of the cerberus gene by Xlim-1, Xotx2, Mix.1, and Siamois, immediately downstream from Nodal and Wnt signaling. *Dev Biol*. 2003; 257:190–204. [PubMed: 12710967]

- Yan YL, Hatta K, Riggleman B, Postlethwait JH. Expression of a type II collagen gene in the zebrafish embryonic axis. *Dev Dyn.* 1995; 203:363–376. [PubMed: 8589433]
- Ybot-Gonzalez P, Cogram P, Gerrelli D, Copp AJ. Sonic hedgehog and the molecular regulation of mouse neural tube closure. *Development.* 2002; 129:2507–2517. [PubMed: 11973281]
- Zhao Q, Behringer RR, de Crombrughe B. Prenatal folic acid treatment suppresses acrania and meroanencephaly in mice mutant for the *Cart1* homeobox gene. *Nat Genet.* 1996; 13:275–283. [PubMed: 8673125]

Author Manuscript

Author Manuscript

Author Manuscript

Author Manuscript

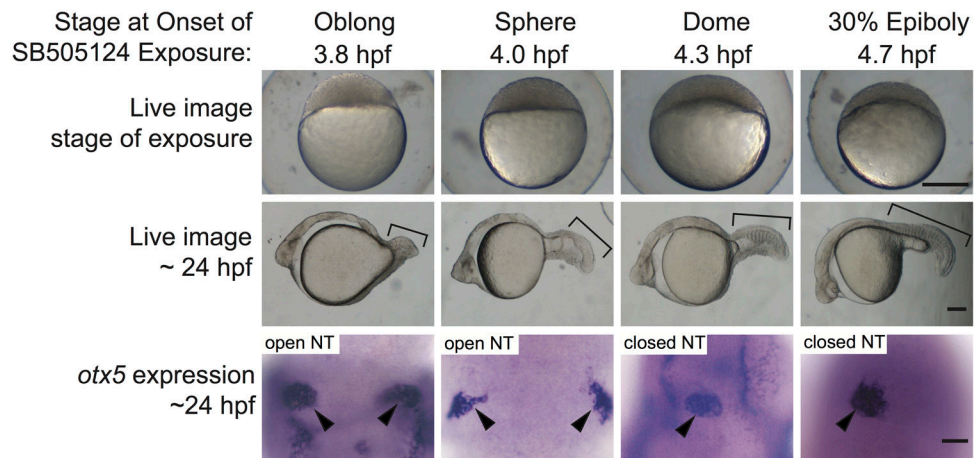


Figure 1. Failure of neural tube closure in embryos treated with the Nodal inhibitor SB505124 for 20 minutes during mid blastula (3.8 and 4.0 hpf)

Embryos treated with 75 μ M SB505124 at all four stages of development have cyclopic eyes. The severity of the defects in mesendodermal/mesodermal derivatives, such as somites (brackets) decreases as the treatments move later in development. Embryos treated for 20 minutes at 3.8 and 4.0 hpf have open neural tubes (open NT), as evidenced by the two domains of pineal precursors (arrowheads). In contrast, embryos treated at 4.3 and 4.7 hpf have oval shaped pineal anlage (arrowheads) indicating a closed anterior neural tube (closed NT). Top row: Lateral views, animal pole to the top, scale bar: 250 μ m. Second row: Lateral views anterior to the left, scale bar: 50 μ m. Third row: Dorsal views anterior to the top. Scale bar: 50 μ m. Refer to Table 1 for quantitative data.

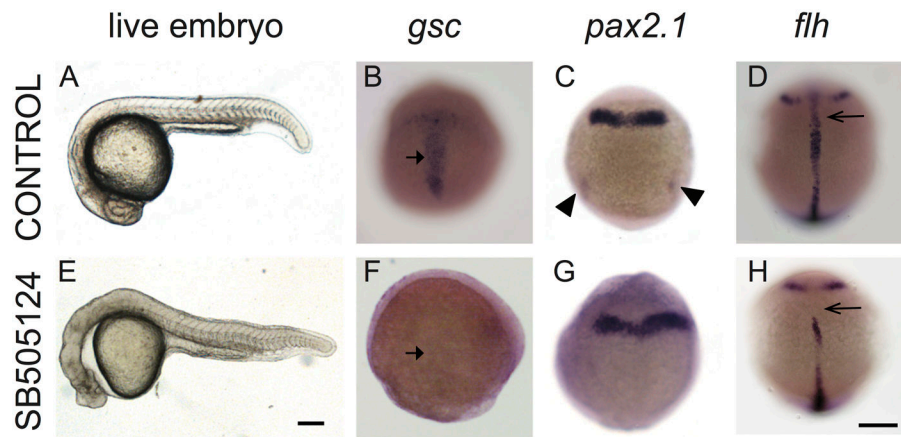


Figure 2. Exposure to Nodal inhibitor SB505124 at 3.8 hpf causes loss of mesendodermal and mesodermal derivatives

(A–D) Control WT embryos exposed to DMSO and (E–H) WT embryos exposed to 50 μ M SB505124. (A) WT embryo at 1 dpf has a normal smooth and round head, a straight body axis, and complete somite formation, while (E) inhibitor treated embryo displays cyclopia and abnormal morphology. (B) Normal *gsc* expression in the prechordal plate of a 9 hpf embryo (90% epiboly) displays a T-shaped expression domain (arrow) that (F) is absent in an inhibitor treated embryo. (C) Normal *pax2.1* expression is present along the midbrain-hindbrain border and in the posterior region in the pronephric mesoderm (arrowheads) in 10 hpf (tailbud stage) embryos. (G) In Nodal deficient embryos, *pax2.1* mRNA is present in the midbrain-hindbrain border (arrowheads) but absent in the pronephric mesoderm. (D) At 12 hpf (6 somite stage), *flh* is expressed in the developing notochord (arrow). (H) SB505124 treated embryos have partial reduction of notochord tissue. Scale bars: 250 μ m.

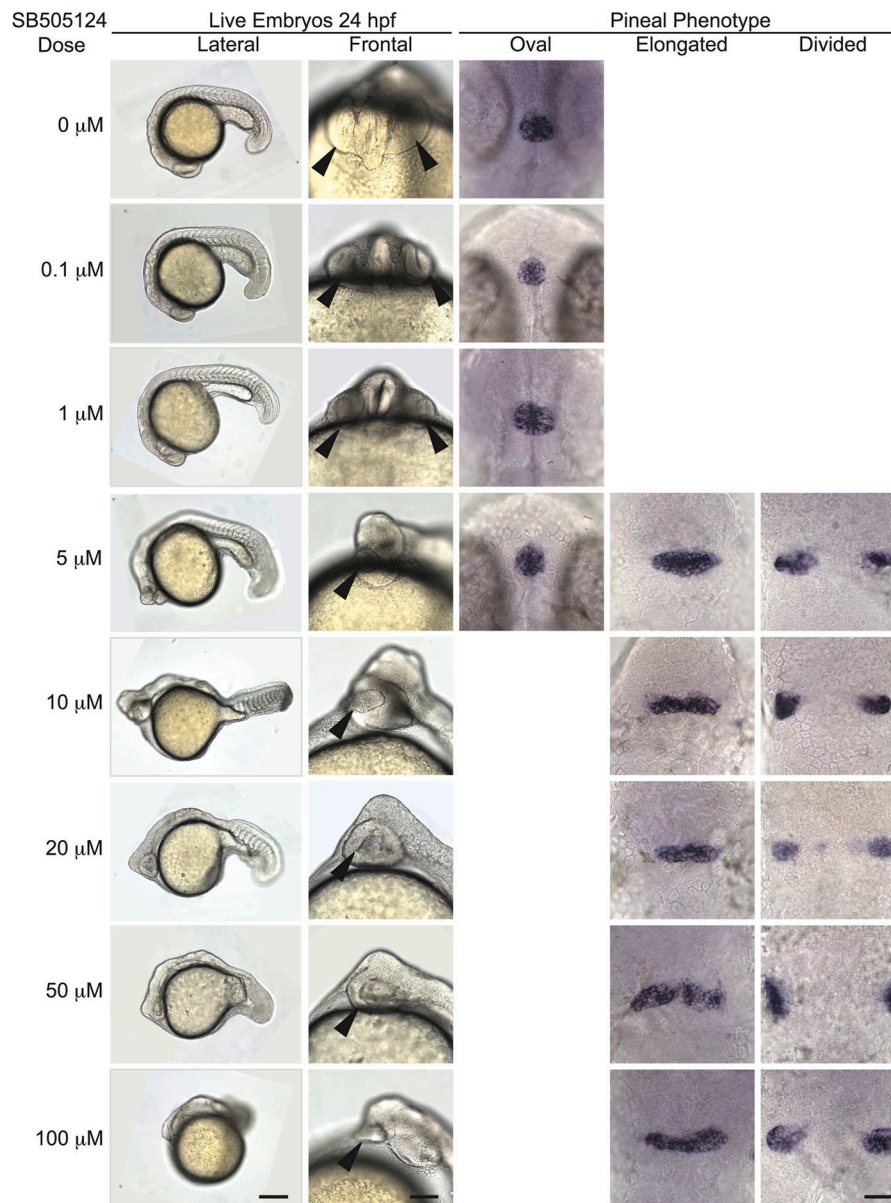


Figure 3. Open neural tube phenotype is fully penetrant upon treatment with SB505124 at concentrations of 10 μ M and higher

All embryos were treated with the indicated concentration of SB505124 at 3.8 hpf (high oblong stage). First column: Anterior to the left and dorsal to the top. Scale bar: 250 μ m. Second column: Anterior to the top. Scale bar: 100 μ m. Arrowheads point to the eye. Third-fifth columns: Embryos were assayed for *otx5* expression in the pineal. Dorsal views, anterior to the top. Scale bar: 50 μ m. Refer to Table 2 for quantitative data.

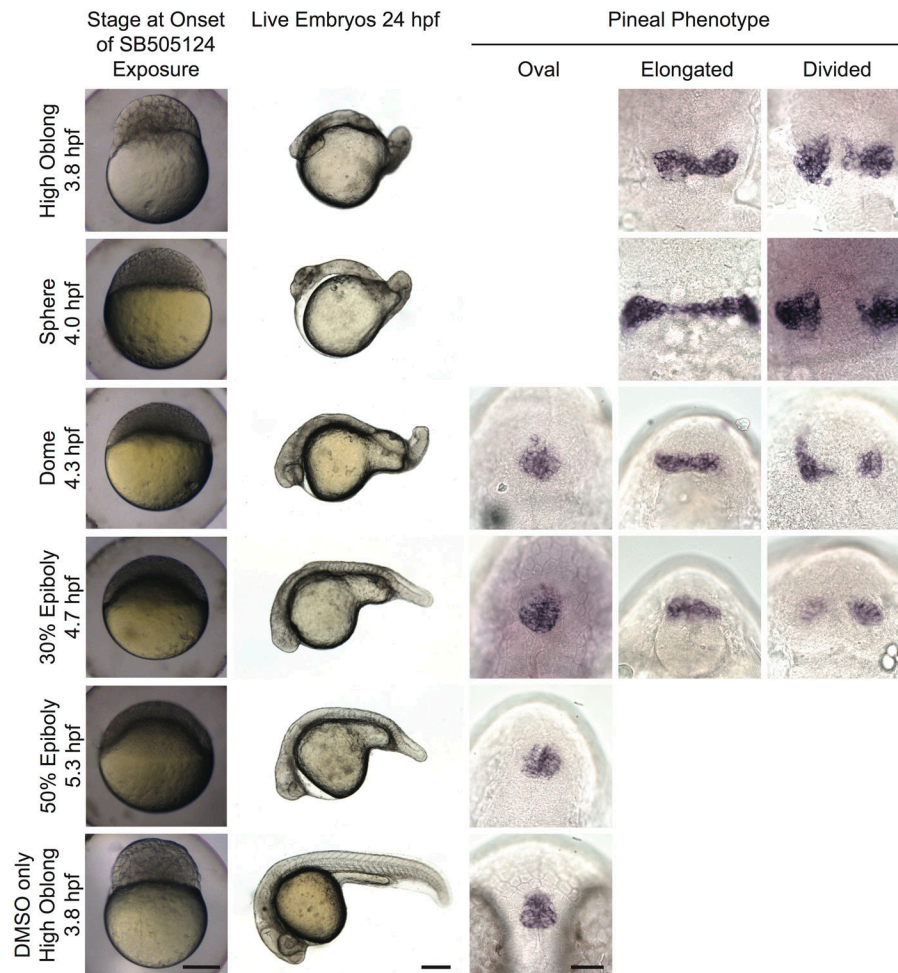


Figure 4. Initiating SB505124 treatment during mid blastula stages blocks neural tube closure
 First column: developmental stage and images of live embryos at the onset of inhibitor exposure. Lateral views with animal pole to the top. Scale bar: 250 μ m. Second column: Lateral views of whole embryos with anterior to the left and dorsal to the top. Scale bar: 250 μ m. Third column: Lateral views of whole embryos with anterior to the left and dorsal to the top. Scale bar: 250 μ m. Third through fifth column: Embryos were assayed for *otx5* expression in the pineal gland. Dorsal views, anterior to the top. Scale bar: 50 μ m. Refer to Table 3 for quantitative data.

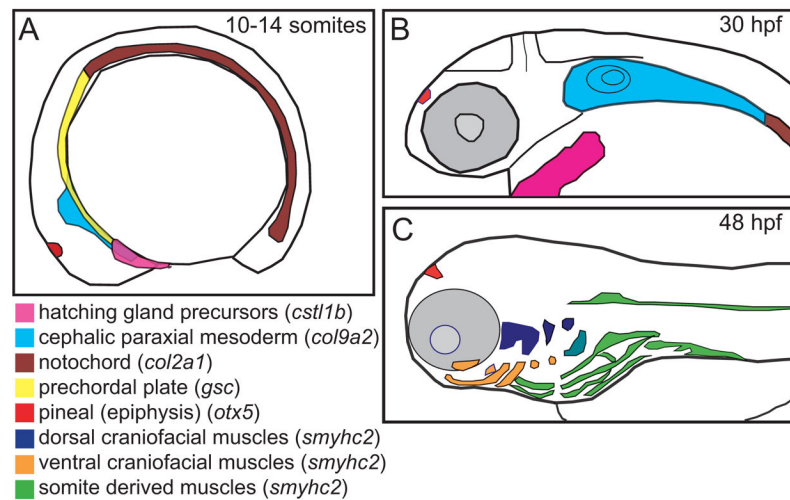


Figure 5. Regions of the head mesendoderm were assayed using a panel of markers
 Schematic representation of expression patterns of mesendodermal and mesodermal tissues along the anterior-posterior axis during (A) the early somite stage, (B) the mid pharyngula period, and (C) the onset of the hatching period. Lateral views, dorsal to the top. Schematics based on published gene expression data (Elworthy *et al.*, 2008; Murakami *et al.*, 2006; Thisse *et al.*, 2001).

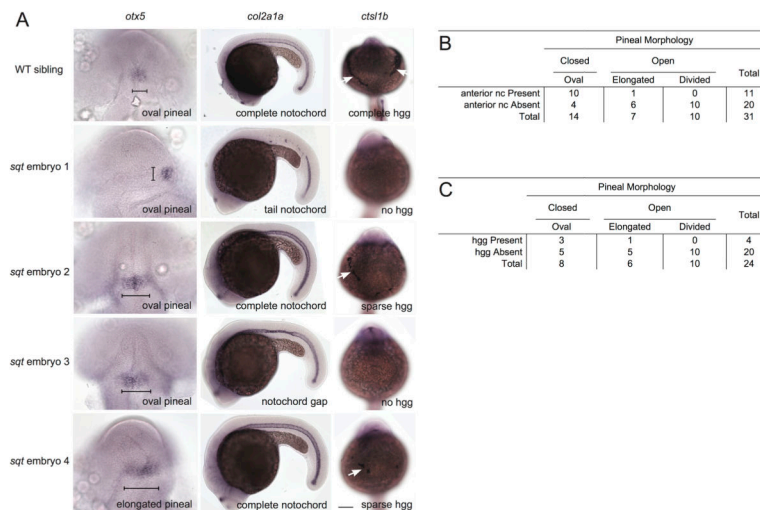
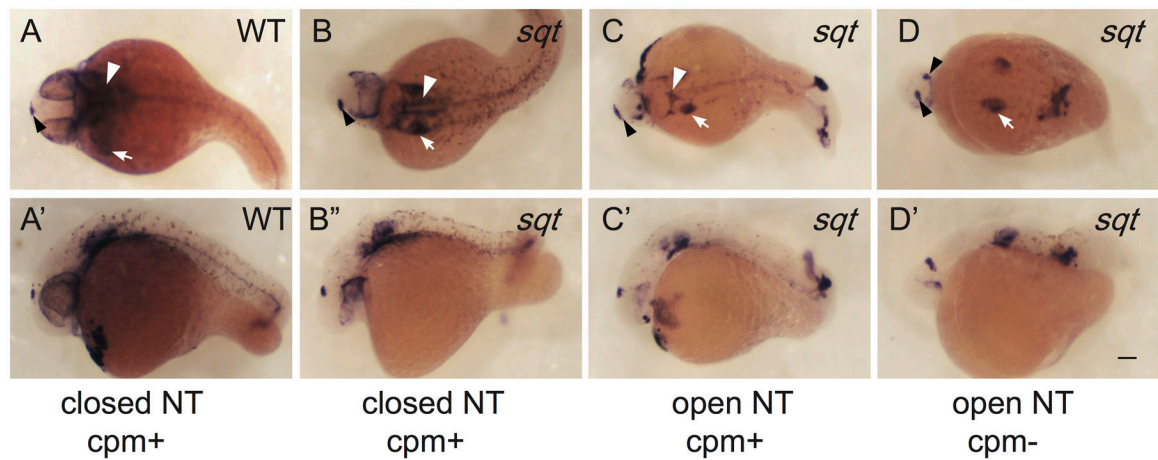


Figure 6. Positive correlation between a closed neural tube closure and the presence of prechordal plate-derived hatching glands and axial mesoderm-derived anterior notochord

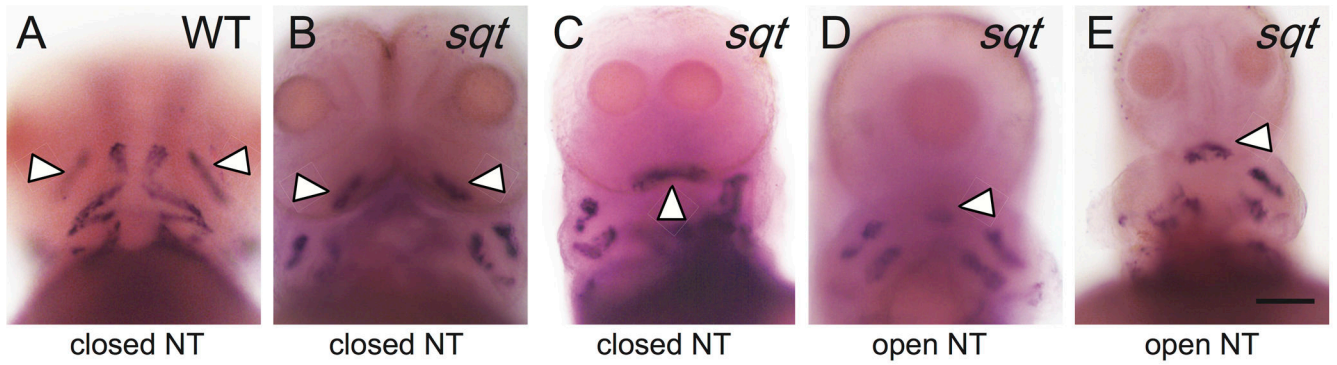
Embryos were raised to ~1 dpf and processed in tandem for *otx5* in the pineal anlage, *col2a1* in the notochord, and *cst11b* in the hatching gland cells (hgg). (A) In WT embryos, the pineal organ is oval indicating a closed neural tube, the notochord spans the complete anterior-posterior extent of the trunk, and the hatching glands make a “necklace” around the anterior of the head. *sqt* embryos have a range of neural tube, notochord, and hgg defects as indicated. Note that, at this stage, *col2a1* is expressed in three adjacent lines of cells, the floor plate (dorsal to the notochord), the hypochord (ventral to the notochord), and the notochord. The gaps in staining in *sqt* embryo 1 correspond to loss of all three tissues. The narrow region of staining in *sqt* embryo 3 just above the hind yolk corresponds to a place where the floor plate and hypochord cells persist, but the wider notochord cells are missing. The neural tube was scored as open if the pineal organ was at least twice as wide along its left-right axis (brackets) compared to its anterior-posterior axis. Images in the same row are different views of the same embryo. First column: Dorsal views with anterior to the top. Second column: Lateral views with anterior to the left and dorsal to the top. Third column: Frontal views with anterior to the top. White arrows point to hatching glands. Scale bars: 100 μ m. (B, C) Complete set of quantitative data.



E

	Pineal Morphology			Total
	Closed	Open		
		Oval	Elongated	
cpm Present	2	3	6	11
cpm Absent	2	1	7	10
Total	4	4	13	21

Figure 7. Correlation between cephalic paraxial mesoderm and neural tube closure
 (A, A') In WT embryos, *col9a2* is expressed in the cpm (white arrowheads) and the ears (white arrow) and the *otx5* expressing pineal anlage (black arrowheads) is oval shaped indicating a closed neural tube. (B–D') *sqt* embryos with different combinations of cpm deficiencies and neural tube phenotypes. (A–D) Dorsal views with anterior to the left and (A'–D') lateral views with anterior to the left and dorsal to the top. Images with the same letter are of the same embryo. (E) Complete set of quantitative data. Scale bar: 100 μ m.



F

	Pineal Morphology			Total
	Closed	Open		
	Oval	Elongated	Divided	
hm Present	12	1	6	19
hm Absent	2	0	2	4
Total	14	1	8	23

Figure 8. Correlation between presence of head muscles and neural tube closure in *sqt* mutants (A–E) WT and *sqt* embryos were raised to 3 dpf and processed in tandem for *smyh2*, in the head muscles (hm) and *otx5*, in the pineal anlage. The adductor mandibulae (am; white arrowheads) are the first muscles to develop in the head region and were used as an indicator for head muscle presence. (A) In WT embryos, am precursors are in two clusters just anterior to the yolk sac and other jaw muscles. The pineal organ is oval indicating a closed neural tube. (B–E) *sqt* embryos with an (B, C) oval pineal with the am present and (D, E) divided pineal with the am present. (F) Complete set of quantitative data. All images are frontal views with anterior to the top. Scale bar: 100 μ m (A–E).

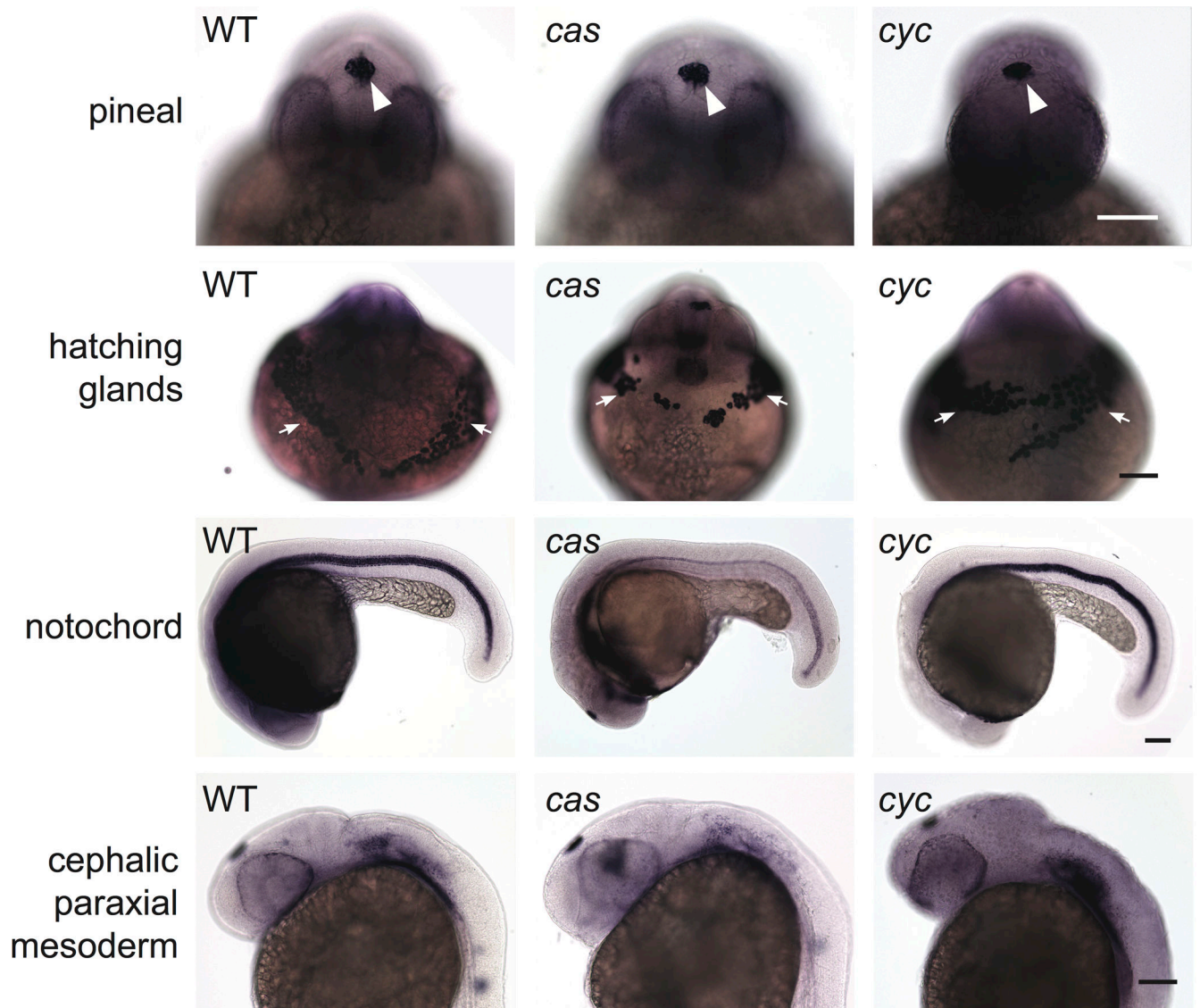


Figure 9. Closed neural tubes and normal mesendoderm/mesoderm development in *cyc* and *cas* mutants

Embryos were co-assayed for *otx5* expression in the pineal precursors and a combination of the following mesendodermal/mesodermal markers: *cts11b* in the hatching glands, *pax 2.1*, *col9a2* in cephalic paraxial mesoderm, and *shh* (for *cas* mutant) or *col2a1* in the notochord (WT embryo and *cyc* mutant). Embryos in the first three rows are at ~26 somite stage and those in the last two rows are 30 hpf. Images in the same column and of the same age are different views of the same embryo. White arrowheads point to pineal, white arrows to hatching glands. Scale bars: 100 μ m.

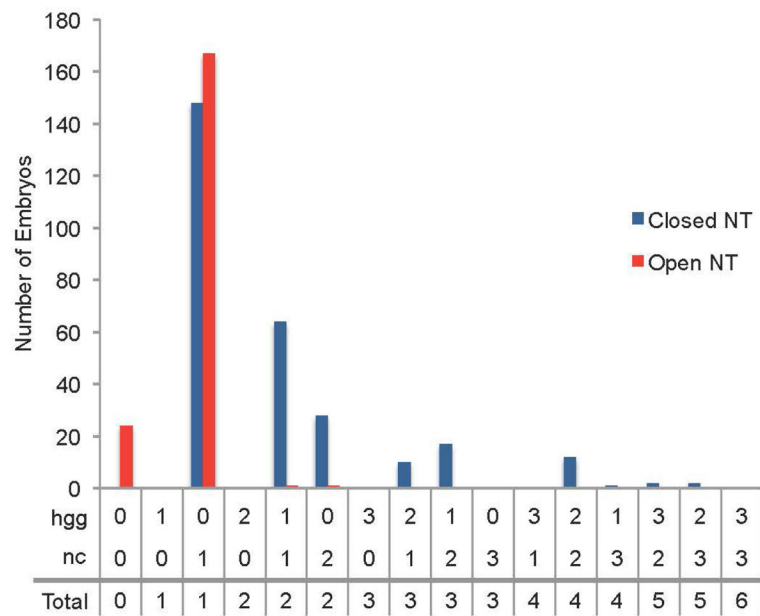


Figure 10. Correlation between total mesendodermal/mesodermal tissue presence and neural tube phenotype

Combination of data from *sqt* mutant embryos and embryos exposed to SB505124 starting at 4.3 hpf. Embryos were fixed at 24 hpf and assayed for neural tube phenotype with *otx5* expression in the pineal. An elongated or divided pineal indicated an open neural tube while an oval pineal indicated a closed neural tube. The presence of the mesendodermal/mesodermal tissues hatching glands (hgg) and whole anterior-posterior notochord (nc) and were labeled with *hgg1* and *col2a1* expression, respectively. These tissues were scored for amount present using the following: 3 = full tissue present, 2 = more than half of tissue present, 1 = less than half of tissue present, 0 = tissue absent.

Treatment of embryos with Nodal inhibitor for 20 minutes at or before 4.3 hpf causes failure in neural tube closure.

Table 1

Stage at Onset of SB505124 Exposure	SB505124 Dose	Closed NT			Open NT		
		Oval Pineal	Elongated Pineal	Divided Pineal	Total		
Oblong (3.8 hpf)	75 μ M	0 (0%)	0 (0%)	6 (100%)	6		
Oblong (3.8 hpf)	100 μ M	0 (0%)	5 (20%)	20 (80%)	25		
Sphere (4.0 hpf)	75 μ M	0 (0%)	2 (9%)	21 (91%)	23		
Sphere (4.0 hpf)	100 μ M	8 (11%)	20 (27%)	46 (62%)	74		
Dome (4.3 hpf)	75 μ M	8 (73%)	0 (0%)	3 (27%)	11		
30% Epiboly (4.7 hpf)	75 μ M	12 (100%)	0 (0%)	0 (0%)	12		
30% Epiboly (4.7 hpf)	100 μ M	6 (100%)	0 (0%)	0 (0%)	6		

Table 2

Increasing penetrance of NTD with increasing dose of Nodal inhibitor.

SB505124 Dose	Closed NT		Open NT	Total
	Oval Pineal	Elongated Pineal	Divided Pineal	
0 μ M	74 (100%)	0 (0%)	0 (0%)	74
0.1 μ M	73 (100%)	0 (0%)	0 (0%)	73
1 μ M	61 (100%)	0 (0%)	0 (0%)	61
5 μ M	36 (55%)	10 (16%)	19 (29%)	65
10 μ M	1 (1%)	8 (11%)	63 (88%)	72
20 μ M	0 (0%)	53 (93%)	4 (7%)	57
50 μ M	0 (0%)	1 (1%)	83 (99%)	84
100 μ M	0 (0%)	1 (2%)	51 (98%)	52

Author Manuscript

Author Manuscript

Author Manuscript

Author Manuscript

Table 3

Initiating treatment of embryos with 100 μ M Nodal inhibitor at or before 4.3 hpf causes open neural tubes.

Stage at Onset of SB505124 Exposure	Closed NT		Open NT		Total
	Oval Pineal	Elongated Pineal	Divided Pineal		
High Oblong (3.8 hpf)	0 (0%)	32 (14%)	199 (86%)		231
Sphere (4.0 hpf)	9 (2%)	85 (18%)	308 (80%)		474
Dome (4.3 hpf)	209 (90%)	17 (8%)	3 (27%)		231
30% Epiboly (4.7 hpf)	452 (98%)	6 (1%)*	5 (1%)*		463
50% Epiboly (5.3 hpf)	178 (99%)	1 (0.05%)	1 (0.05%)		180

* The small number of embryos with open neural tubes in the 30% epiboly time point were likely slightly younger embryos that contaminated those samples.

Author Manuscript

Author Manuscript

Author Manuscript

Author Manuscript